



HAL
open science

Impact of neovascular age-related macular degeneration on eye-movement control during scene viewing: Viewing biases and guidance by visual salience

Antje Nuthmann, Miguel Thibaut, Thi Ha Chau Tran, Muriel Boucart

► To cite this version:

Antje Nuthmann, Miguel Thibaut, Thi Ha Chau Tran, Muriel Boucart. Impact of neovascular age-related macular degeneration on eye-movement control during scene viewing: Viewing biases and guidance by visual salience. *Vision Research*, 2022, 201, pp.108105. 10.1016/j.visres.2022.108105 . hal-03814569

HAL Id: hal-03814569

<https://cnrs.hal.science/hal-03814569v1>

Submitted on 14 Oct 2022

HAL is a multi-disciplinary open access archive for the deposit and dissemination of scientific research documents, whether they are published or not. The documents may come from teaching and research institutions in France or abroad, or from public or private research centers.

L'archive ouverte pluridisciplinaire **HAL**, est destinée au dépôt et à la diffusion de documents scientifiques de niveau recherche, publiés ou non, émanant des établissements d'enseignement et de recherche français ou étrangers, des laboratoires publics ou privés.

1
2 **Impact of neovascular age-related macular degeneration on eye-movement control**
3 **during scene viewing: viewing biases and guidance by visual salience**
4

5
6 Antje Nuthmann¹, Miguel Thibaut², Thi Ha Chau Tran^{2,3}, and Muriel Boucart²
7

8
9 ¹Institute of Psychology, University of Kiel, Kiel, Germany

10 ²University of Lille, Lille Neuroscience & Cognition, INSERM, Lille, France

11 ³Ophthalmology Department, Lille Catholic Hospital, Catholic University of Lille, Lille,
12 France
13

14
15 Antje Nuthmann  <http://orcid.org/0000-0003-3338-3434>

16 Thi Ha Chau Tran  <https://orcid.org/0000-0001-9066-7092>

17 Muriel Boucart  <https://orcid.org/0000-0001-7112-990X>

18 Correspondence concerning this article should be addressed to Antje Nuthmann,
19 University of Kiel, Institute of Psychology, Olshausenstr. 62, 24118 Kiel, Germany, or
20 Muriel Boucart, Faculty of Medicine, Pôle Recherche, 1 place de Verdun, 59000 Lille,
21 France, or via e-mail: nuthmann@psychologie.uni-kiel.de or muriel.boucart@chru-lille.fr.
22

23
24
25
26
27
28
29
30
31
32
33
34
35
36
37
38
39
40
41
42
43
44
45
46
47
48
49

Abstract

Human vision requires us to analyze the visual periphery to decide where to fixate next. In the present study, we investigated this process in people with age-related macular degeneration (AMD). In particular, we examined viewing biases and the extent to which visual salience guides fixation selection during free-viewing of naturalistic scenes. We used an approach combining generalized linear mixed modeling (GLMM) with a-priori scene parcellation. This method allows one to investigate group differences in terms of scene coverage and observers' well-known tendency to look at the center of scene images. Moreover, it allows for testing whether image salience influences fixation probability above and beyond what can be accounted for by the central bias. Compared with age-matched normally sighted control subjects (and young subjects), AMD patients' viewing behavior was less exploratory, with a stronger central fixation bias. All three subject groups showed a salience effect on fixation selection—higher-salience scene patches were more likely to be fixated. Importantly, the salience effect for the AMD group was of similar size as the salience effect for the control group, suggesting that guidance by visual salience was still intact. The variances for by-subject random effects in the GLMM indicated substantial individual differences. A separate model exclusively considered the AMD data and included fixation stability as a covariate, with the results suggesting that reduced fixation stability was associated with a reduced impact of visual salience on fixation selection.

233 words

keywords:

Macular degeneration; eye movements; naturalistic scenes; saliency; individual differences

50

51 **1 Introduction**

52 Patients suffering from advanced stages of age-related macular degeneration (AMD)
53 have to rely on their peripheral vision to explore their surroundings and to perform tasks (see
54 Verghese et al., 2021, for a review). Common complaints of patients with AMD (or more
55 generally low vision) seeking visual rehabilitation are problems associated with reading,
56 driving and face recognition (Cahill et al., 2005; Rubin, 2013; Taylor et al., 2016). Moreover,
57 research has shown that AMD patients often suffer from fixation instability and poor
58 oculomotor control (Crossland, Crabb, et al., 2011; Kumar & Chung, 2014). Therefore, it is
59 perhaps unsurprising that few studies have investigated how AMD patients actively explore
60 naturalistic scenes through eye movements. With the present work, we start to fill this gap by
61 investigating eye guidance during free-viewing of real-world scenes in AMD patients as
62 compared with normally sighted older and young adults. Primarily, we wanted to explore
63 whether effects of visual salience on saccade target selection were preserved in patients with
64 AMD.

65 When viewing a scene, we make sequences of saccades and fixations (Malcolm et al.,
66 2016). Saccades are quick ballistic movements that bring the eyes to new parts of the scene.
67 During fixations, the eyes are relatively still to allow visual processing of the scene stimulus.
68 From a given fixation in the scene, there are many potential locations for the next fixation.
69 Even without taking the current scene into account, fixation locations are not randomly
70 selected. Among the regularities or “biases” in the manner in which we explore scenes, is the
71 bias to fixate at or near the center of an image (central bias, Mannan et al., 1996; Tatler,
72 2007). Various factors contribute to the central bias (Rothkegel et al., 2017, for a review),
73 among them strategic components. In particular, the center of the screen may be an optimal
74 location for extracting information from scenes (Tatler, 2007).

75 The saccades we make during scene viewing are also biased: we make more
76 horizontal eye movements than vertical ones, with oblique saccades being the least frequent
77 (horizontal bias, Foulsham et al., 2008). The roots of the horizontal bias are still under
78 investigation (Anderson et al., 2020; Foulsham & Kingstone, 2010). Given that the horizontal
79 bias is already present in infants, it may be related to the asymmetry in the topography of
80 human photoreceptors (Van Renswoude et al., 2016). According to another account, the
81 distribution of image features may guide eye movements in a bottom-up manner toward the
82 image horizon (Foulsham et al., 2008).

83 The saccade target selection process is also guided by the visual salience of the scene
84 stimulus, in particular during free-viewing of scene images (Parkhurst et al., 2002; Peters et
85 al., 2005). Guidance by visual salience means that the eyes are directed to scene regions
86 based on image features generated in a bottom-up manner from the scene. These features,
87 which tend to be correlated (Baddeley & Tatler, 2006; Nuthmann & Einhäuser, 2015),
88 include luminance, contrast, edge density, and color (Mannan et al., 1996; Tatler et al., 2005).
89 Different feature maps are combined in a saliency map (e.g., Itti et al., 1998), where brighter
90 values indicate higher visual salience (see Figure 1b and c). Eye guidance by image features
91 assumes that the eyes are directed to the most salient location in the map first, followed by an
92 eye movement to the next most salient location, and so on. Due to the photographer's bias in
93 scene composition, salience tends to be higher in the center of scenes (Tatler, 2007), calling
94 for statistical methods that allow for assessing the independent contributions of visual
95 salience and center bias to fixation selection in scenes (Nuthmann et al., 2017).

96 Saliency map models are models of visual attention rather than models of eye-
97 movement control (see Frintrop et al., 2010, for a review), which may explain why most of
98 them do not distinguish between visual salience in central vision as opposed to the periphery.
99 Empirical eye-movement studies, on the other hand, have highlighted the importance of
100 peripheral vision for the saccade target selection process. The importance of a given region of
101 the visual field to a process or task can be assessed by implementing gaze-contingent
102 artificial scotomas, which continuously remove (or strongly degrade) scene information in a
103 selected region (e.g., David et al., 2019; Nuthmann, 2014).

104 For example, Nuthmann (2014) asked observers to search for a medium-sized target
105 object in each scene. One of her six scotoma conditions simulated the absence of central
106 vision. With only peripheral vision available, participants were able to direct their eyes to the
107 object, and their initial landing positions on the object gave rise to a two-dimensional
108 Gaussian distribution with a peak close to the center of the object (i.e., the Preferred Viewing
109 Location, PVL, Nuthmann & Henderson, 2010). **In other words**, the PVL was preserved
110 when observers' central vision was **artificially impaired**. **This finding shows** the importance
111 of peripheral vision in fixation selection.

112 Moreover, Nuthmann (2014) used the eye-movement data to decompose the button-
113 press search times into **three phases representing** particular sub-processes of search (Malcolm
114 & Henderson, 2009). The data **showed the following** dissociation in behavior: **Participants**
115 **with a simulated central scotoma**¹ were selectively impaired in verifying the identity of the
116 target, but not locating it. **In contrast, the same participants with a simulated peripheral**

117 scotoma were selectively impaired in locating the target, but not identifying it (see also
118 Nuthmann et al., 2021). **The data suggest** a central-peripheral dichotomy **in which** peripheral
119 vision **selects** and central vision **recognizes** (Zhaoping, 2019).

120 AMD leads to a central scotoma due to which foveal or central analysis is impaired.
121 As a result, the ability of people with AMD to correctly identify objects and scenes is reduced
122 (Thibaut et al., 2015). However, patients' remaining peripheral vision has shown to be
123 sufficient for object and scene categorization (Boucart et al., 2013; Tran et al., 2010). For
124 example, Tran et al. (2010) showed that individuals with a central scotoma were able to
125 categorize scenes displayed for 300 ms as natural/urban or indoor/outdoor with high accuracy
126 (> 75% correct), even though their performance was below that of normally sighted controls.
127 The results from categorization studies (see also Boucart et al., 2008; Tran et al., 2012)
128 suggest that individuals with AMD are able to quickly recognize the overall meaning or
129 "gist" of the scene.

130 In a more naturalistic setting, the rapid recognition of the scene's gist is supplemented
131 by active scene exploration, for which people with AMD may adopt an eccentric viewing
132 strategy. Eccentric viewing involves directing the eye such that the image falls onto still
133 functioning parts of the retina. The region of retina used is referred to as the preferred retinal
134 locus (PRL) or pseudo-fovea (Crossland, Engel, et al., 2011; Cummings et al., 1985;
135 Timberlake et al., 1986).

136 In the present study, we asked participants to free-view images of naturalistic scenes.
137 Thus, participants were given no specific instructions other than to look at the images. With
138 our main analysis, we tested how "active" AMD patients' scene viewing behavior is, and
139 how prone they are to the central fixation bias. Importantly, the analysis also allowed us to
140 test whether image salience has an independent effect on fixation selection. We hypothesized
141 that AMD patients explore fewer scene regions and exhibit a stronger center bias, due to
142 problems with oculomotor control (see Verghese et al., 2021). Critically, assuming that the
143 peripheral selection of the next fixation location follows similar guidance principles in AMD
144 patients and normally sighted individuals, we expected to observe similar effects of image
145 salience on fixation probability for the two subject groups. In a complementary analysis, we
146 also investigated whether the horizontal bias was preserved in AMD patients.

147 We compared the eye-movement data of the AMD patients with data from age-
148 matched, normally sighted older participants. Additionally, we included a group of young
149 adults to dissociate the effects of pathology **and** normal ageing. Results from previous studies
150 suggest that the effect of location-based visual salience on fixation probability is smaller for

151 older adults compared with young adults (Açik et al., 2010; Nuthmann et al., 2020).
152 Moreover, it was found that young and older adults show similar levels of explorative
153 viewing behavior (Açik et al., 2010) and no differences in central bias (Nuthmann et al.,
154 2020).

155 For our main analysis, we used an approach combining generalized linear mixed
156 modeling (GLMM) with a-priori scene parcellation (Nuthmann et al., 2017; Nuthmann et al.,
157 2020). This method allows us to investigate group differences in terms of scene coverage,
158 central bias and—**crucially**—the importance of image salience for fixation selection **in** scene
159 viewing.

160 When conducting experiments, researchers are mainly interested in the average
161 response to independent variables or predictor variables. Existing variability across subjects
162 is typically treated as error variance (Cronbach, 1957), potentially obscuring differences
163 between levels of an independent variable of interest (Vogel & Awh, 2008). However, this
164 approach ignores many relevant sources of inter-subject variability, including the use of
165 different strategies for the same task (Seghier & Price, 2018). Between-participant variance
166 can differ considerably between populations. Groups of older adults often (but not always)
167 show higher inter-subject variability than younger adults (Rabbitt, 1993; Shammi et al.,
168 1998). Moreover, patient groups can have a high degree of heterogeneity (e.g., Wolfers et al.,
169 2020).

170 When finding a group-level effect, it **can be informative** to explore the role played by
171 factors associated with the individual. For example, in studies with AMD patients it is
172 common to correlate a measure of their visual disability with their average score in a
173 dependent variable of interest (e.g., Thibaut et al., 2016; Thibaut et al., 2015; Tran et al.,
174 2010; Wiecek et al., 2012). In recent years, mixed-effects models have proved to be a
175 particularly suitable tool for assessing individual differences (Kliegl et al., 2011; Rouder &
176 Haaf, 2019). One particular advantage of mixed-effects models is that they allow one to make
177 statistical inferences about experimental effects and individual differences on the basis of a
178 single analysis. Therefore, a secondary aim of the present study is to demonstrate the use of
179 GLMM for documenting reliable individual differences with regard to scene-viewing
180 parameters in different subject groups.

181 2 Methods

182 2.1 Participants

183 The participants whose data we report in the present article took part in a larger study
184 consisting of several tasks. The eye-tracking results from an object search task have been
185 published elsewhere (Thibaut et al., 2020). The study was approved by the ethics committee
186 for behavioral sciences at the University of Lille (N°EUDRACT 2010-101088-31) and was
187 conducted in accordance with the tenets of the Declaration of Helsinki. All participants gave
188 their written informed consent. The AMD patients and the age-matched control subjects were
189 both recruited in the department of ophthalmology at the Saint-Vincent de Paul Hospital in
190 Lille, France. The young observers were recruited among medical students and psychology
191 students at the university.

192 Patients suffering from neovascular AMD with subfoveal involvement and with best
193 corrected visual acuity (BCVA; i.e., acuity measured with subjective refraction) between 0.3
194 to 1 logMAR were included. They were treated with at least three monthly ranibizumab
195 intravitreal injections prior to participating in the experiments. Clinical assessment included
196 visual acuity measurement, funduscopy, and optical coherence tomography (OCT). BCVA
197 was measured at a distance of 4 m using the ETDRS chart, which was converted to logMAR
198 visual acuity.

199 Fluorescein angiography, indocyanine green angiography (ICGA), and spectral
200 domain OCT (Heidelberg Retina Angiograph, HRA2; Heidelberg Engineering, Dossenheim,
201 Germany) were used to confirm the diagnosis of neovascular AMD and to determine the size
202 of the lesion (cf. Querques et al., 2012). With fluorescein angiography, the lesion area was
203 defined as containing choroidal neovascularization, hemorrhages, scar tissue and serous
204 pigment epithelial detachment. The ICG plaque was defined as an area of late
205 hyperfluorescence seen in ICGA. The area of the lesion (mm²) and the greatest linear
206 diameter of the lesion (mm) were then measured by outlining the lesion using the Eye
207 Explorer image analysis software (Heidelberg Engineering, Heidelberg, Germany).
208 Microperimetry was not performed as several patients had very low vision (P4, P7, P10) or
209 were too old (above 80 years) for such a long clinical test.

210 A French version of the Mini Mental State Examination (MMSE) was **conducted** to
211 **assess** cognitive impairment in the AMD **patients** and in the **age-matched normally sighted**
212 **control subjects**. **We excluded** participants with a history of neurologic **or psychiatric** disease,

213 cognitive impairment (MMSE < 25) or significant ocular diseases **that** might compromise
214 oculomotor function.

215 Clinical assessment and experiments were performed during the same visit. The eye-
216 tracking data from 17 patients diagnosed with AMD (14 women; mean age 78.2 ± 4.3 years)
217 and 17 age-matched normally sighted controls (11 women; mean age 76.9 ± 7.2 years) were
218 included for the present analyses. Note that 32 AMD patients were meant to be included, but
219 the data from 15 patients had to be excluded due to excessive head movements, poor
220 validation results for the calibration of the eye tracker, or data loss during eye-movement
221 recordings (Thibaut et al., 2020). Additional data came from 17 young normally sighted
222 controls (8 women; mean age 23.8 ± 2.5 years).

223 **Eye movements were recorded** monocularly. **For** patients with bilateral AMD, the eye
224 with the best-corrected visual acuity **was used**. If both eyes had equal acuity, **we selected** one
225 eye randomly. **For** young and older control **subjects**, their preferred eye **was tracked**. **Note**
226 **that viewing was monocular**, with the non-tracked eye being occluded throughout
227 calibrations and recordings.

228 Table 1 provides the individual demographic and clinical data for the AMD patients
229 included in the study. The mean duration of the disease was three years, ranging from three to
230 98 months. Note that the variables describing patients' visual ability (visual acuity, greatest
231 linear diameter of the lesion, and surface area of the lesion) are highly correlated with one
232 another (Spearman's rank correlations: $r \geq 0.87$, $p < 0.001$). A few patients had training in
233 eccentric viewing, to varying extents.

234 -----
235 Insert Table 1 about here
236 -----

237 **2.2 Apparatus**

238 Eye-tracking equipment by SensoMotoric Instruments (SMI, Teltow, Germany) was
239 used. Eye movements were recorded with a tower-mount iViewX Hi-Speed eye tracker with
240 a 350 Hz sampling rate (AMD patients, age-matched controls) and a portable RED-m eye
241 tracker at 120 Hz (young participants). Both eye trackers offer comparable accuracy and
242 precision. According to the manufacturer, the typical accuracy is 0.25 to 0.5° for the iViewX
243 eye tracker, and 0.5° for the RED-m eye tracker. Eye-movement event detection took the
244 differences in eye-tracker sampling rate into account.

245 The eye tracker was calibrated using a 5-point calibration procedure, followed by a 5-
246 point calibration accuracy test. Subjects were asked to look at black discs (radius: 1°) that

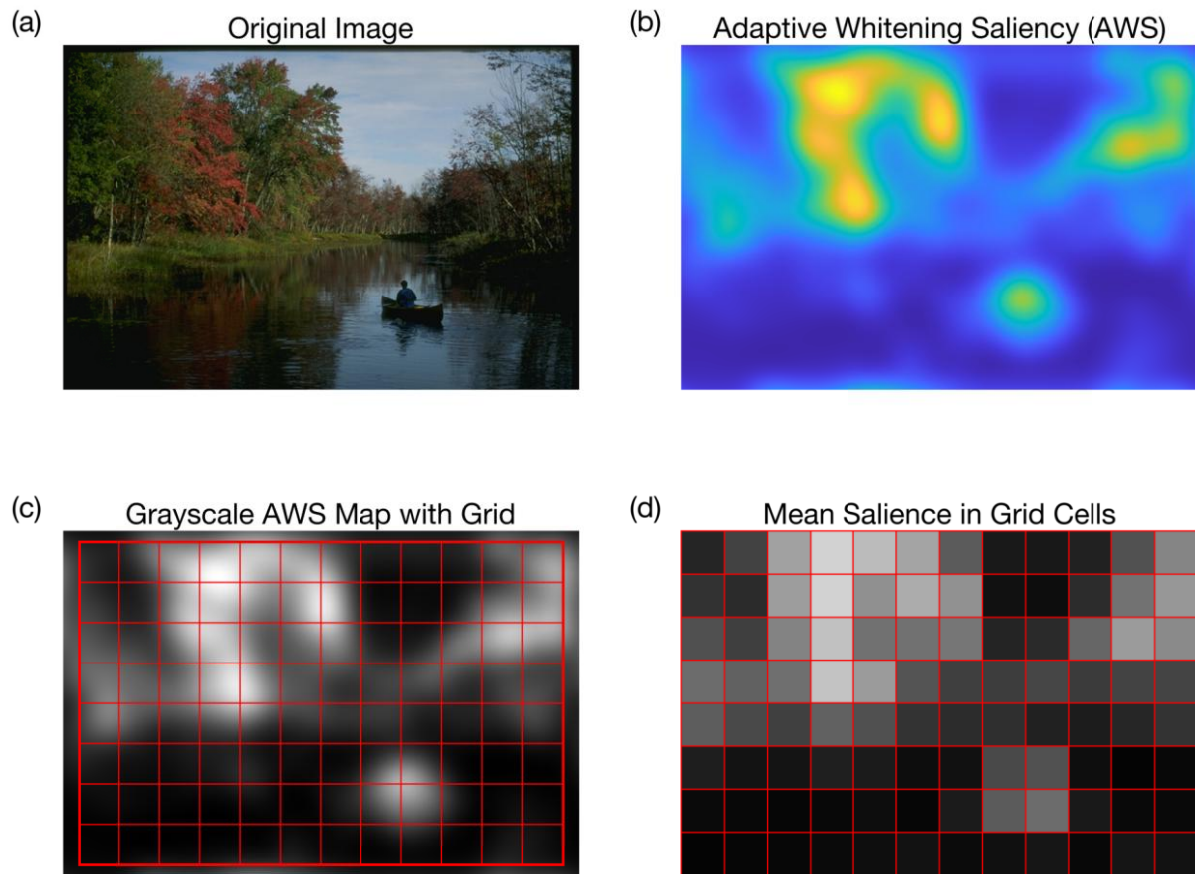
247 appeared sequentially on the screen. The first calibration target was presented at the center of
248 the screen, whereas the other ones were presented in random order in each of the four
249 quadrants of the screen. The AMD patients fixated the calibration targets with their fovea or
250 PRL (cf. Vullings & Verghese, 2021), see the Discussion section for additional
251 considerations.

252 **2.3 Design, stimuli, and procedure**

253 The experiment was run using the Experiment Center software (SMI). First,
254 participants' fixation stability was evaluated. To this end, participants were asked to fixate a
255 black dot (radius: 1°) centrally displayed for 10 seconds on a light grey background.
256 Afterwards, each participant free-viewed 20 color photographs of real-world outdoor scenes,
257 15 of which contained at least one person (see Figure 1a for an example). Each scene image
258 was presented once for 10 s. Scene presentation was randomized across participants in each
259 group. Each trial began with the presentation of a central cross for one second, which
260 participants were instructed to fixate. Following a gap of 200 ms, the scene image was
261 presented.

262 Scenes were displayed on a 17-inch Dell monitor with a screen resolution of $1280 \times$
263 1040 pixels (width \times height). Scene images had an original resolution of 1024×683 pixels
264 and were scaled up to 1280×854 pixels in the experiment. At a viewing distance of 60 cm,
265 images subtended a visual angle of $36.3^\circ \times 29.5^\circ$. Images came with a small black framing.
266 The analysis grid spanned the central 1200×800 pixels and thereby discounted the black
267 surrounding.

268



269
270

271 Figure 1. (a) One of the **scene** images used in the study. (b) A saliency map (Adaptive
272 Whitening Saliency) for this image. (c) The same AWS map in grayscale, with the analysis
273 grid overlaid in red. In panels (b) and (c), brighter **regions** indicate higher visual saliency. (d)
274 Mean saliency values for the grid cells, color-coded using the gray colormap.
275

276 2.4 Data analysis

277 For a given participant, the gaze raw data from the scene viewing experiment were
278 converted into a fixation sequence matrix and a saccade sequence matrix using the BeGaze
279 software (SMI). For oculomotor event detection, the software's low-speed event detection
280 method was used. With this method, the detector first searches for fixation events, after
281 which saccade events are computed. To identify fixations, the detector uses a dispersion-
282 based algorithm (cf. Salvucci & Goldberg, 2000), for which the default settings were used. In
283 particular, the minimum fixation duration was set to 80 ms.

284 The **fixation** data were further processed and analyzed in MATLAB (The
285 MathWorks, Natick, MA) and the R system for statistical computing. The figures were

286 created with MATLAB (Figure 1) or with the *ggplot2* (version 3.3.5, Wickham, 2016) and
287 *cowplot* (Wilke, 2020) R packages.

288 Fixation probabilities and fixation counts were analyzed with generalized mixed-
289 effects models (GLMMs). Continuous response variables, in particular fixation durations and
290 saccade amplitudes, were analyzed using linear mixed-effects models (LMMs). Fixation
291 durations were log-transformed prior to inclusion in the LMM (Nuthmann, 2017). The
292 mixed-model analyses were conducted with the R package *lme4* (version 1.1-27.1, Bates et
293 al., 2015), using the `glmer` function for GLMMs and the `lmer` function for LMMs. For
294 LMMs, *p* values for fixated effects were obtained using Satterthwaite approximation as
295 implemented in the *lmerTest* R package (version 3.1.3, Kuznetsova et al., 2017). For a
296 technical introduction to mixed models in R, see Demidenko (2013). A tutorial is provided by
297 Brown (2021).

298 **2.4.1 Grid method**

299 To assess the independent effect of visual salience on fixation probability, each scene
300 image was parcellated into local image regions. As in previous research, we used a grid with
301 equal-sized, square cells (Nuthmann & Einhäuser, 2015; Nuthmann et al., 2017; Nuthmann et
302 al., 2020). How fine or coarse should the grid be? The problem with a very fine grid is that
303 the trial-based observation matrix may contain too many zeros (cf. Nuthmann et al., 2017).
304 The research question sets an upper bound for the grid cell size—it is implausible to
305 investigate fixation guidance by visual salience with a very coarse grid. For the present
306 analyses, we chose a 12×8 (width \times height) parcellation (Figure 1c), yielding 96 quadratic
307 cells, with each cell spanning $2.8^\circ \times 2.8^\circ$ (100×100 pixels).

308 Next, we mapped the empirical eye-fixation data onto the scene analysis grid. We
309 constructed an observation matrix based on the experimental design and the fixation data.
310 The complete observation matrix would comprise 97,920 rows (3 subject groups \times 17
311 subjects per group \times 20 images \times 96 grid cells per image). There were seven missing trials,
312 reducing the observation matrix accordingly. In previous applications of the grid method, the
313 grid cell on which the very first fixation in a given trial fell was excluded from analysis (e.g.,
314 Nuthmann & Einhäuser, 2015). For the present analysis, this grid cell was included if it
315 received immediate refixations and/or later revisits. This procedure was adopted to guard
316 against underestimating the central bias, in particular for AMD patients. Fixation probability
317 was measured by a binary response variable: for a given subject and image, it was coded
318 whether a given grid cell was fixated (1) or not (0).

319 2.4.2 Computation of saliency maps and central bias

320 Over the years, many different saliency models have been developed (Borji & Itti,
321 2013), for some of which the code is available publicly (e.g., Wloka et al., 2018). Following
322 related work (Nuthmann et al., 2020), we used the Adaptive Whitening Saliency (AWS)
323 Model (Garcia-Diaz et al., 2012). For each image, a corresponding saliency map was
324 generated using code provided by the authors. The default parameters were used, with one
325 exception: The output scaling factor (default value: 0.5) was set to 1.0 to compute saliency
326 maps at full image resolution. The saliency map of each image was then normalized to the
327 same range, arbitrarily chosen as [0,1] (Nuthmann et al., 2017). Supplementary Fig. 1 shows
328 the mean normalized saliency map for the 20 scene images used in the study.

329 Local salience can be defined as the mean or the maximum (peak) over the saliency
330 map's values within each grid cell. The correlation between mean and peak AWS across all
331 grid cells from all images was very high, $r = 0.927$, $p < 0.001$. For the present analyses we
332 chose the mean (see Figure 1d for a visualization), because it tends to be the more robust
333 measure (Nuthmann et al., 2017; Nuthmann et al., 2020).

334 To account for observers' central bias of fixation, the GLMM included a central-bias
335 predictor along with the salience predictor. How should the central-bias predictor be
336 calculated? An intuitive solution is to determine the Euclidean distance from image center
337 (e.g., Nuthmann & Einhäuser, 2015). The Euclidean distance-to-center variable is an
338 isotropic measure, assuming equal spread of fixation positions in the horizontal and vertical
339 dimensions. However, fixation positions in scene viewing often show a horizontal-vertical
340 anisotropy (Clarke & Tatler, 2014). To decide about which central-bias variable to use, we
341 took a data-driven approach (Nuthmann et al., 2017). In particular, we specified one-
342 predictor GLMMs to test the seven central-bias predictors proposed by Nuthmann et al.
343 (2017). For a given central-bias variable, one model considered the combined data from all
344 three subject groups. Three additional models were run to analyze the data from each subject
345 group separately. The more negative the standardized regression coefficient for the fixed
346 effect central bias, the more variance is explained by the tested central-bias predictor
347 (potentially leaving less variance to explain for the salience predictor). The numeric ranking
348 of central-bias predictors differed across subject groups, but within a group the confidence
349 intervals for the seven estimated central-bias effects overlapped. Further explorations
350 revealed that AMD patients showed little anisotropy, compared with the other two groups.
351 Numerically, the taxicab predictor performed best for the patient group. It was also chosen

352 for the present analyses because it was less sensitive to differences in anisotropy between
353 groups, compared with other isotropic central-bias measures. The taxicab predictor was
354 generated by calculating the distance between each grid cell center and the center of the
355 image along the horizontal and vertical image axes:

$$356 \quad C_{g,taxicab} = |x_g - x_c| + |y_g - y_c|. \quad (1)$$

357 **2.4.3 Statistical analysis using mixed models**

358 **In our main analysis, we used** generalized linear mixed models (Bolker et al., 2009;
359 Jaeger, 2008) to model fixation probability in scenes for three different subject groups. **The**
360 **data were** modeled at the level of individual observations (i.e., the zeros and ones). We used
361 the logit transformation of the probability, which the `glmer` function uses by default for
362 binary data. **Using the logit link function means that** parameter estimates are obtained on the
363 log-odds or logit scale. **This scale** is symmetric around zero and ranges from negative to
364 positive infinity. **A logit of 0 corresponds to a probability of 0.5;** negative log-odds **indicate**
365 probabilities **smaller than 0.5.**

366 Mixed models incorporate both fixed-effects parameters and random effects. The
367 GLMM included nine fixed effects (intercept, two main effects, six interaction coefficients).
368 The two stimulus-related fixed effects were image salience and central bias. Stimulus-related
369 input variables were measured within participants on a continuous scale. For the GLMM
370 analyses, **they were z transformed to a mean of 0 and a standard deviation of 1.** Subject group
371 is a categorical variable. To include subject group as predictor in the GLMM, contrast coding
372 was used (see below). Differences between subject groups were tested through interactions
373 between “subject group” and a given continuous predictor.

374 Random effects represent subjects’ or items’ deviations from the fixed-effect
375 parameters; they are assumed to be normally distributed with a mean of 0 (Baayen et al.,
376 2008). In our study design, the random factor “subject” is nested under “subject group”,
377 because each subject can only belong to one subject group. Subjects and scenes are crossed
378 random effects, because every subject saw all 20 scene items.

379 Because we were particularly interested in individual differences, the GLMM was set
380 up to include the “maximal” structure (Barr et al., 2013) for the random factor “subject”.
381 Thus, the random-effects structure comprised a by-subject random intercept, random slopes
382 for central bias and salience, and three correlation parameters. This allowed us to explore the
383 degree to which subjects differed in their responses above and beyond belonging to their
384 subject group, which was modelled as a fixed effect. If there are genuine differences between

385 individuals, including by-subject random effects should lead to an improvement in model fit
386 (see Staub, 2020).

387 Results from previous research on eye-movement control during scene viewing
388 suggest that item variances are much larger than subject variances (Nuthmann & Einhäuser,
389 2015; Nuthmann et al., 2017). Therefore, the random-effects structure of the GLMM also
390 included the maximal structure for the random factor “scene item”.

391 Using Wilkinson notation (Wilkinson & Rogers, 1973), the model formula for the
392 main GLMM reported in this article was:

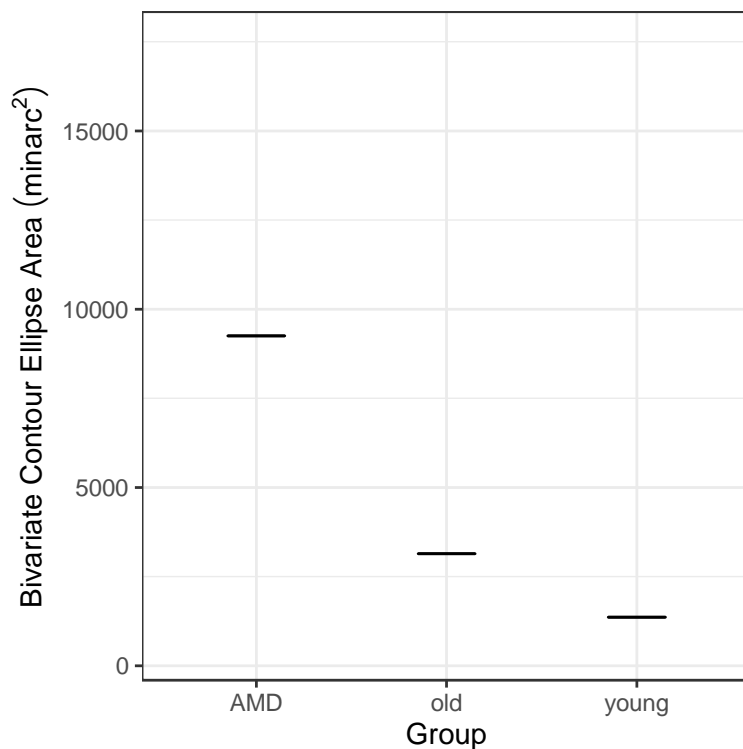
393 $\text{Fixated} \sim 1 + \text{SubjectGroup} + \text{CentralBias} + \text{CentralBias}:\text{SubjectGroup} + \text{Saliency} +$
394 $\text{Saliency}:\text{SubjectGroup} + (1 + \text{CentralBias} + \text{Saliency} | \text{Subject}) + (1 + \text{CentralBias} + \text{Saliency}$
395 $| \text{Scene}).$ (2)

396 **3 Results**

397 First, we report the results from the fixation stability test. Second, we characterize
398 subjects’ eye-movement behavior during scene viewing at a basic level. Third, we report
399 results from our main analysis exploring whether individuals with AMD differ from age-
400 matched control subjects (and young subjects) in terms of scene coverage and central bias
401 and regarding the importance of image saliency for fixation selection during scene viewing.
402 Fourth, we report results from a complementary analysis, in which we explored another
403 viewing bias; that is, the horizontal bias.

404 **3.1 Fixation stability**

405 Fixation stability was quantified by using the conventional method of calculating the
406 Bivariate Contour Ellipse Area (BCEA) introduced by Steinman (1965) with parameters used
407 by Crossland et al. (2004). A larger BCEA value is indicative of a less stable fixation. The
408 results are presented in Figure 2 (for the AMD patients, see also Table 1). Our a priori
409 hypotheses were as follows: fixation stability should be worse for AMD patients than for age-
410 matched control subjects (Rohrschneider et al., 1995); moreover, fixation stability may be
411 better for young than for older adults (Altemir et al., 2022). One-sided unpaired two-sample
412 Wilcoxon tests confirmed these predictions. The BCEA (in minarc^2) for the AMD patients
413 ($Mdn = 9250$, $IQR = 10422$) was significantly larger than the BCEA for the age-matched
414 controls ($Mdn = 3143$, $IQR = 5663$), $W = 213$, $p = 0.009$. In contrast, the BCEA for the young
415 adults ($Mdn = 1363$, $IQR = 1389$) was significantly smaller than the BCEA for the control
416 group of older adults, $W = 61$, $p = 0.002$.



418

419 Figure 2. Fixation stability data for AMD patients, age-matched normally sighted subjects,
 420 and young adults. Each dot presents an individual participant's Bivariate Contour Ellipse
 421 Area (BCEA) value. The horizontal lines represent the medians for the three subject groups.
 422 Lower BCEA values indicate better fixation stability.

423

424 3.2 Basic Eye-Movement Measures

425 To provide a basic description of subjects' eye movements during scene viewing, we
 426 calculated the mean number of fixations per trial, along with mean fixation durations and
 427 saccade amplitudes (Table 2). Specifically, means or counts were calculated for each subject,
 428 and these were then averaged across subjects of a given group. The data were analyzed with
 429 mixed models, without prior averaging. Each model included the factor subject group as a
 430 fixed effect and random intercepts for subjects and scene items. To assess the effect of
 431 subject group, dummy coding (also referred to as treatment coding) was used, with the
 432 control group of old participants serving as the reference level. This coding created two
 433 contrasts, which allowed for testing whether there were any differences (a) between AMD
 434 patients and the control group or (b) between young and old participants.

435 The number of fixations per trial (count variable) was modeled using a Poisson
 436 GLMM with a log link function. The two contrasts were not significant (AMD - control: $b = -$

437 0.043, $SE = 0.09$, $z = -0.48$, $p = 0.633$; young - old: $b = -0.036$, $SE = 0.09$, $z = -0.4$, $p =$
438 0.691). Fixation duration and saccade amplitude (continuous variables) were analyzed with
439 LMMs. For log-transformed fixation durations, the two planned contrasts were not significant
440 (AMD - control: $b = -0.083$, $SE = 0.099$, $t = -0.84$, $p = 0.406$; young - old: $b = 0.113$, $SE =$
441 0.099 , $t = 1.14$, $p = 0.260$). Saccade amplitudes were significantly reduced for AMD patients
442 compared with age-matched controls, $b = -1.423$, $SE = 0.4$, $t = -3.56$, $p < 0.001$. Mean
443 saccade amplitudes were not significantly different for young compared with old adults, $b =$
444 0.504 , $SE = 0.399$, $t = 1.26$, $p = 0.213$. In summary, the main finding from these analyses is
445 that AMD patients made saccades with shorter amplitudes than age-matched normally
446 sighted subjects.

447 -----
448 Insert Table 2 about here
449 -----

450 3.3 GLMM results: Central bias and image salience

451 Next, we conducted a grid-based mixed-model analysis to assess effects of image
452 salience on fixation selection, after controlling for subjects' tendency to look at the center of
453 scene images. Using mixed modeling allows one to simultaneously investigate group
454 differences and individual differences.

455 3.3.1 Group-level effects

456 To include the predictor subject group in the GLMM, a dummy-coding scheme was
457 used. Consequently, the GLMM did not test main effects (i.e., average effects across the three
458 subject groups) but simple effects; that is, effects for the reference group of old participants.
459 Importantly, differences between the three subject groups were tested through interactions.
460 For example, including the interaction between salience and subject group allowed for testing
461 whether the salience effect was significantly different for either of the other two subject
462 groups. The actual coefficient for the effect of salience in AMD patients (or young
463 participants) is obtained by adding the simple effect coefficient and the relevant interaction
464 coefficient. The GLMM results are summarized in Table 3, with the fixed-effects results
465 depicted in Figure 3.

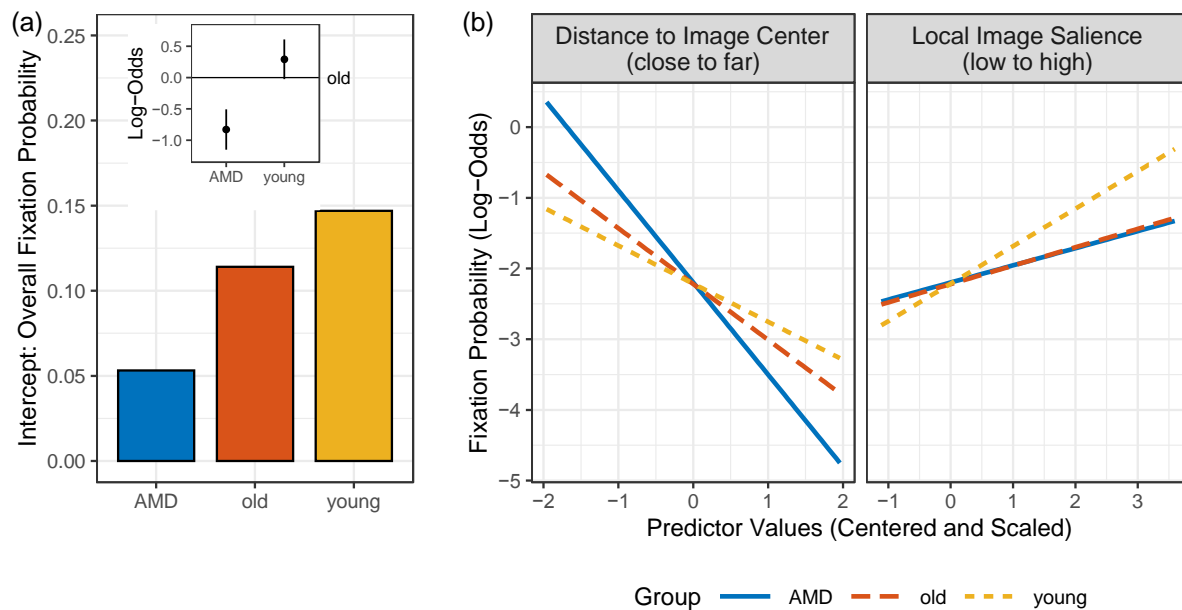
466 The first fixed effect in the GLMM is the intercept. It represents the overall fixation
467 probability, describing how many different scene patches observers selected for fixation. The
468 fixed effect for the model intercept characterizes the group of older adults: $b = -2.049$, $SE =$
469 0.122 , $z = -16.83$, $p < 0.001$. Note that the logit value of -2.049 corresponds to a probability

470 of 0.114. The fact that the intercept was significantly different from zero has no interpretative
471 meaning. Compared to the reference group of older adults, the intercept was significantly
472 lower for AMD patients ($b = -0.830$, $SE = 0.164$, $z = -5.04$, $p < 0.001$), indicating that AMD
473 patients fixated fewer scene patches than age-matched old observers. There was no
474 significant difference between old and young adults ($b = 0.291$, $SE = 0.162$, $z = 1.8$, $p =$
475 0.072). The intercept coefficient for the AMD patients is the sum of the coefficient for the old
476 subjects (-2.049) and the interaction coefficient (-0.830). The interaction coefficient is a
477 difference score, describing the difference between AMD patients and old subjects. Figure 3a
478 provides a visualization.

479 The central-bias predictor describes how fixation probability varies as a function of
480 distance from scene center. A significant negative slope for the reference group (older adults)
481 captures the well-known central bias (Mannan et al., 1996; Tatler, 2007); that is, fixation
482 probability linearly decreased with increasing distance from scene center ($b = -0.772$, $SE =$
483 0.094 , $z = -8.18$, $p < 0.001$). Compared to the reference group of older adults, the central-bias
484 slope was significantly more negative for AMD patients ($b = -0.534$, $SE = 0.128$, $z = -4.16$, p
485 < 0.001) and less negative for young adults ($b = 0.256$, $SE = 0.126$, $z = 2.03$, $p = 0.043$).
486 Thus, the central bias was most pronounced for AMD patients, who showed an increased
487 tendency to fixate central regions of the image. The central bias was weakest for young
488 adults, with older adults in between.

489 Importantly, our GLMM based grid cell analysis allowed for assessing to what degree
490 image salience influences fixation selection above and beyond a general preference for
491 fixating the center of the image. For the reference group (older adults) there was a significant
492 positive fixed effect for AWS, which means that fixation probability increased with
493 increasing image salience of the image regions ($b = 0.245$, $SE = 0.072$, $z = 3.40$, $p = 0.001$).
494 Young adults showed a significantly stronger effect of image salience than older adults ($b =$
495 0.25 , $SE = 0.079$, $z = 3.17$, $p = 0.002$), which is in agreement with previous research (Açik et
496 al., 2010; Nuthmann et al., 2020). Interestingly, there was no significant difference between
497 AMD patients and older adults ($b = -0.008$, $SE = 0.08$, $z = -0.1$, $p = 0.923$).

498 -----
499 Insert Table 3 about here
500 -----
501



502

503 Figure 3. Fixed-effects results from the grid GLMM fitting fixation probability during scene
 504 viewing for AMD patients, old normally sighted control subjects, and young subjects. (a)
 505 Intercept, representing the overall fixation probability (converted from log-odds to
 506 probabilities). The brown bar depicts the intercept for the old subjects (reference group). The
 507 inset plot shows two difference scores: the difference between AMD patients and old subjects
 508 (AMD – old) and the difference between young and old subjects (young – old), with the error
 509 bars depicting 95% confidence intervals. Accordingly, the intercept for the AMD patients
 510 (blue bar) and/or young subjects (yellow bar) is derived by summing the simple effect
 511 coefficient for the old subjects and the respective difference score. (b) Predicted partial
 512 effects of central bias (left) and image saliency (right) on fixation probability in log-odds
 513 scale for AMD patients (blue solid line), age-matched normally sighted subjects (brown long-
 514 dashed line), and young adults (yellow dashed line). The predictions were generated with the
 515 `keepEF` function from the *remefR* package (Hohenstein & Kliegl, 2020).

516

517 To test the generalizability of results, a number of control analyses were performed.
 518 First, local saliency was defined as the grid cell’s peak saliency rather than its mean saliency.
 519 Second, the binary response variable (1 fixated, 0 not fixated) was replaced with fixation
 520 counts, which were modeled using a poisson GLMM with a log link function. Third, we
 521 repeated all analyses with a coarse 6×4 grid. The qualitative pattern of results did not
 522 change.²

523 3.3.2 Individual differences

524 The GLMM was set up with the maximal random-effects structure to protect against
525 Type I errors (Barr et al., 2013; Schielzeth & Forstmeier, 2009). However, by including by-
526 subject and by-item random effects we can also account for individual differences and item
527 effects (Nuthmann et al., 2017). Here, we will use the GLMM results to assess whether there
528 were reliable individual differences, which we expected to be particularly pronounced among
529 the AMD patients.

530 To recapitulate, by-subject random effects represent subjects' deviations from the
531 fixed-effect parameters. Accordingly, the zero lines in Figure 4a represent the fixed-effect
532 estimates. Specifically, the vertical broken line in both panels of Figure 4a represents the
533 model intercept. The horizontal broken lines represent the central-bias effect (left panel) and
534 the salience effect (right panel), respectively. The dots in Figure 4a depict the by-subject
535 random effects, with different colors denoting different subject groups. The horizontal and
536 vertical error bars depict 95% prediction intervals.

537 For all three variables of interest, there are quite a few subjects for which the
538 prediction intervals do not include the zero line (Figure 4a). For some of the subjects,
539 particularly AMD patients, the prediction intervals are entirely on opposite sides of the zero
540 line. Thus, the graphs are suggestive of considerable individual differences.

541 To test whether the differences between individuals were statistically reliable, the
542 maximal model (Table 3) was compared with two reduced models. In model 1, the by-subject
543 random slope capturing the central bias and the two correlation parameters involving the
544 central bias were removed. In model 2, the by-subject random slope capturing the salience
545 effect and the two correlation parameters involving image salience were removed.

546 Likelihood ratio tests (LRT) were used to determine whether dropping a particular
547 random effect from the maximal model led to a significantly worse fit of the model. The log-
548 likelihood increases with goodness of fit. The Akaike Information Criterion (AIC, Akaike,
549 1974) corrects the log-likelihood statistic for the number of estimated parameters. The
550 Bayesian Information Criterion (BIC, Schwarz, 1978) additionally corrects for the number of
551 observations. The AIC and BIC both decrease as goodness of fit increases.

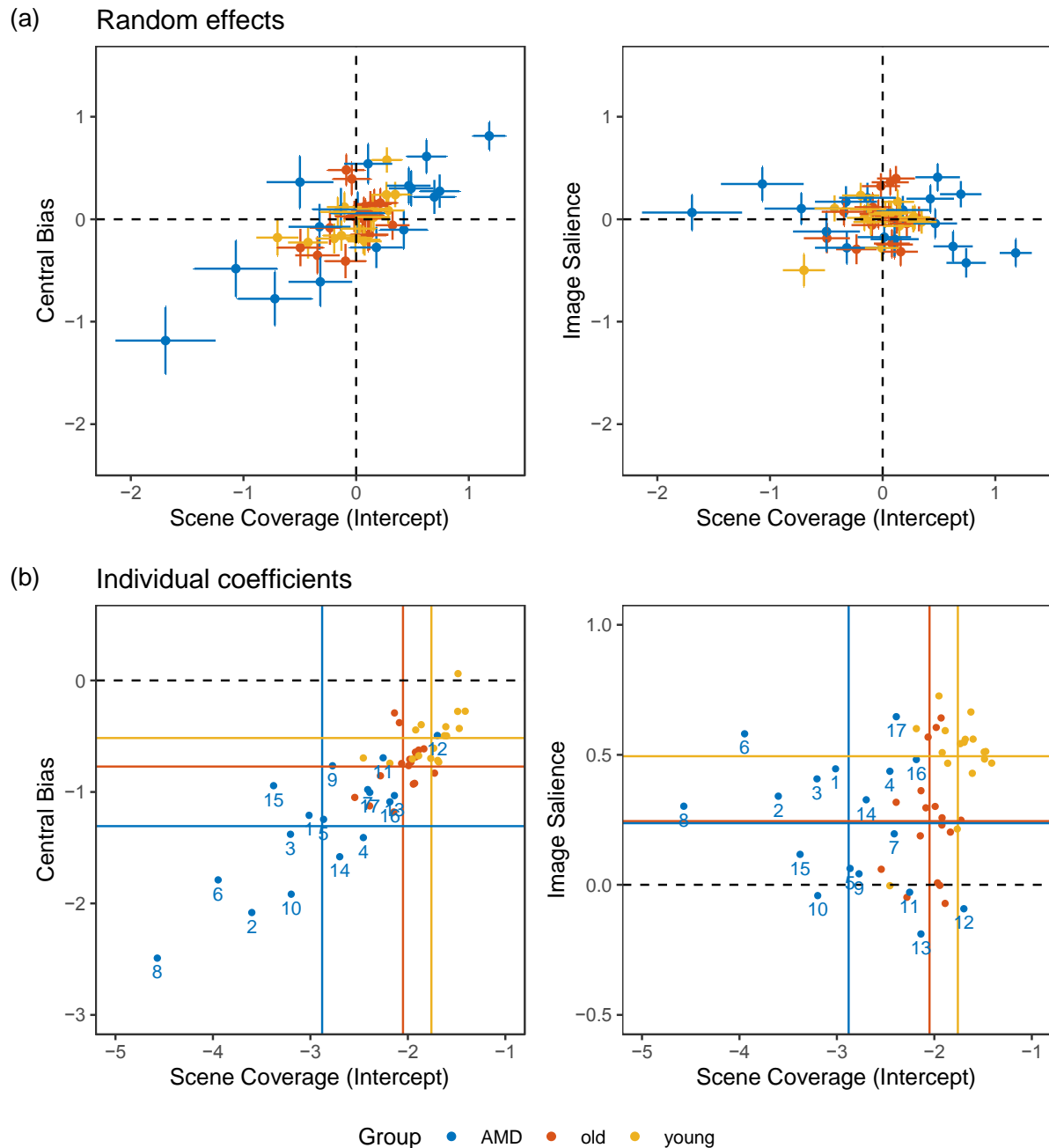
552 According to the LRT, model 1 provided a significantly worse goodness of fit than
553 the maximal model ($\log\text{Lik } \Delta\chi^2(3) = 584.66, p < 0.001$); moreover, both AIC and BIC were
554 larger for model 1 than for the maximal model (AIC: $68685 - 68106 = 579$; BIC: $68855 -$
555 $68305 = 550$).

556 Model 2 also provided a significantly worse goodness of fit than the maximal model
557 ($\log\text{Lik } \Delta\chi^2(3) = 402.9, p < 0.001$), with both AIC and BIC being larger for model 2 than for
558 the maximal model (AIC: $68503 - 68106 = 397$; BIC: $68674 - 68305 = 369$). Put the other
559 way around, including by-subject random slopes (and the corresponding correlation
560 parameters) in the maximal model led to an improvement in model fit. In summary, the
561 model comparisons substantiate that there were genuine differences between individuals.

562 To obtain individual subject coefficients for a given variable of interest, we need to
563 add the predictions for random effects to the fixed-effect estimate. In Figure 4b, the
564 differently colored dots depict the individual coefficients for the 51 subjects from the three
565 different subject groups. For the 17 AMD patients, represented by the blue dots, the subject
566 numbers from Table 1 are additionally provided. Moreover, the colored horizontal and
567 vertical lines represent the fixed-effect estimates for the three variables and three subject
568 groups.

569 To reiterate, the central bias describes the phenomenon that fixation probability
570 decreases with increasing distance from image center. Therefore, almost all subject
571 coefficients for the central-bias predictor are negative (Figure 4b, left). The more negative the
572 central-bias coefficient, the stronger the central bias. The intercept represents the overall
573 fixation probability. A smaller by-subject intercept means that fewer scene patches were
574 fixated, and this is associated with a stronger central fixation bias. The systematic
575 relationship between intercept and central bias is particularly evident for the AMD patients,
576 with some of them showing a particularly strong central bias.

577 The salience effect captures the observation that fixation probability tends to increase
578 with increasing image salience. Therefore, most subject coefficients for the salience predictor
579 are positive (Figure 4b, right). However, some of the individual coefficients are negative or
580 close to zero, which means that salience had no impact on fixation selection for these
581 subjects. For example, AMD patient 10 shows a relatively strong central bias and no salience
582 effect. AMD patient 8, on the other hand, shows low scene coverage and a strong central
583 bias, but an average salience effect.



584

585 Figure 4. By-subject effects on fixation probability for the 51 subjects that took part in the
 586 study. Scatterplots of the central-bias effect (left panels) and the saliency effect (right panels)
 587 against the intercept in the GLMM. The intercept represents the overall fixation probability; a
 588 small by-subject intercept indicates that few scene patches were fixated (i.e., scene coverage
 589 was low). In each panel, different colors denote subjects that belong to a given subject group
 590 (blue: AMD, brown: age-matched old adults, yellow: young adults). (a) The conditional
 591 modes of the distributions of random effects are shown by colored dots, given the
 592 observations and evaluated at the parameter estimates. The horizontal and vertical error bars
 593 depict 95% prediction intervals. (b) Individual subject coefficients; that is, the sum of fixed-

594 effect estimates and predictions for random effects. The colored vertical lines depict the
595 fixed-effect estimates for the intercept in the GLMM for a given subject group. The colored
596 horizontal lines depict the fixed-effect estimates for central bias (panel b, left) and salience
597 (panel b, right) for a given subject group.

598

599 **3.3.3 Inclusion of patient variables as fixed effects in the GLMM**

600 A final question we considered is whether there is a systematic relationship between
601 AMD patients' visual ability and indicators of fixation selection in scenes. An intuitive
602 solution may be to compute correlations between measures of patients' visual ability (Table
603 1) and their GLMM subject coefficients (Figure 4b). Kliegl et al. (2011) point out that
604 random effects for different subjects are not independent observations. For this reason, the
605 authors advise not to use random effects (or individual coefficients) for further inferential
606 statistics, and to refer to estimates of (G)LMM parameters instead. Accordingly, we
607 evaluated the AMD patients' fixation data in another GLMM for which the fixed-effects
608 structure comprised the central-bias and salience predictors, and also a "patient variable" and
609 its interactions with central bias and salience. The model equation was as follows:

610 $\text{Fixated} \sim 1 + \text{CentralBias} + \text{Salience} + \text{PatientVariable} + \text{PatientVariable:CentralBias} +$
611 $\text{PatientVariable:Salience} + (1 + \text{CentralBias} + \text{Salience} \mid \text{Subject}) + (1 + \text{CentralBias} +$
612 $\text{Salience} \mid \text{Scene}).$ (3)

613 For the predictor reflecting patients' visual ability we chose the surface area of the
614 lesion (Table 1). We reasoned that a larger central scotoma may lead to a less effective use of
615 peripheral vision and therefore to less exploratory viewing behavior and weaker guidance by
616 visual salience. However, the main effect of surface area on fixation probability was not
617 significant, $b = 0.142$, $SE = 0.197$, $z = 0.72$, $p = 0.472$. The interaction between surface area
618 and central bias was also not significant, $b = 0.02$, $SE = 0.146$, $z = 0.14$, $p = 0.892$. The
619 interaction between surface area and salience was not significant either, $b = -0.047$, $SE =$
620 0.067 , $z = -0.7$, $p = 0.485$.

621 There was no systematic relationship between patients' scotoma size (surface area)
622 and their BCEA value (Spearman's rank correlation: $r = 0.14$, $p = 0.600$), which is in
623 agreement with previous research (e.g., Crossland, Culham, et al., 2004). Note that the results
624 from reading studies suggest that higher BCEA values are associated with decreases in
625 reading speed (e.g., Crossland, Culham, et al., 2004; Rubin & Feely, 2009). Therefore, we
626 conducted an exploratory mixed-model analysis with predictors related to AMD patients'

627 BCEA values as fixed effects. This analysis allowed us to explore the relationship between
628 patients' fixation stability and indicators of fixation selection. The main effect of fixation
629 stability on fixation probability was not significant, $b = 0.135$, $SE = 0.198$, $z = 0.68$, $p =$
630 0.494 . The interaction between fixation stability and central bias was also not significant, $b =$
631 0.028 , $SE = 0.146$, $z = 0.19$, $p = 0.848$. However, there was a significant interaction between
632 fixation stability and salience, $b = -0.155$, $SE = 0.056$, $z = -2.77$, $p = 0.006$, which means that
633 higher BCEA values (indicating lower fixation stability) were associated with a smaller
634 salience effect.³

635 **3.4 Horizontal bias**

636 When inspecting complex scenes, observers not only show a central bias, but also a
637 horizontal bias; that is, a preference for horizontal over vertical and oblique saccades
638 (Foulsham et al., 2008). In a complementary analysis, we therefore explored whether the
639 horizontal bias was preserved in AMD patients.

640 The direction of a saccade was quantified as the angle between the horizontal plane
641 and the line connecting the current fixation with the next fixation. For a given subject group,
642 a polar histogram was constructed by sorting saccade angles from all observers into 36
643 equally spaced bins of 10° . The density histograms in Figure 5a show the expected horizontal
644 bias. The saccade-angle distributions for AMD patients and age-matched control subjects
645 showed no substantial differences. However, it appears that young adults made saccades
646 along the horizontal plane ($\pm 5^\circ$) more frequently than older adults and AMD patients.

647 For statistical evaluation, the proportion of horizontal, vertical, and oblique saccades
648 was calculated for each subject in a given group (cf. Van Renswoude et al., 2016). Saccades
649 made along the 0° axis and the 180° axis ($\pm 30^\circ$) were classified as horizontal saccades,
650 whereas saccades made along the 90° axis and the 270° axis ($\pm 30^\circ$) were classified as vertical
651 saccades. Finally, saccades made along the 45° , 135° , 225° , and 315° axes ($\pm 15^\circ$) were
652 classified as oblique saccades. Thus, each of the three directional categories (horizontal,
653 vertical, oblique) covered the same angular range (i.e., 120°).

654 For a given subject group, about 50% of the saccades were classified as horizontal
655 saccades (AMD patients: 48.7%, age-matched controls: 49.7%, young adults: 51.9%); see
656 Figure 5b. The proportion of horizontal saccades did not differ between AMD patients and
657 age-matched controls, $t(32) = -0.41$, $p = 0.688$. Using broadly defined categories, the
658 proportion of horizontal saccades did not differ significantly between young and older adults

659 either, $t(32) = 0.9, p = 0.374$. None of the other two-sample t -tests indicated significant
 660 differences.



661
 662 Figure 5. Analysis of the angular direction of saccades. (a) Distribution of saccade directions
 663 for AMD patients (blue solid line), age-matched normally sighted subjects (brown long-
 664 dashed line), and young adults (yellow dashed line). The polar histograms depict densities
 665 and were constructed using a bin size of 10° . The dots represent the bin centers. A 90°
 666 saccade angle denotes an upward saccade, 180° a leftward saccade, and 270° a downward
 667 saccade. The solid radial grid lines denote the cut-off points to classify horizontal, vertical,
 668 and oblique saccades; see text for additional details. (b) Proportion of horizontal, vertical, and
 669 oblique saccades for the three subject groups. Each dot presents an individual participant's
 670 proportion, and horizontal lines represent the mean. For a given subject group, the three mean
 671 proportions add up to 1.

672

673 4 Discussion

674 The purpose of this study was to investigate where and how AMD patients look at
 675 images of naturalistic scenes. Our analyses focused on viewing biases and the impact of
 676 visual salience. Compared with age-matched normally sighted subjects, AMD patients'

677 viewing behavior was less exploratory, with a stronger central fixation bias. Both subject
678 groups showed an independent effect of image salience on fixation probability. The salience
679 effect was not reduced in AMD patients, suggesting that eye guidance by visual salience was
680 still intact. The horizontal bias was also preserved in the patient group.

681 In our scene viewing task, each trial started with the presentation of a central fixation
682 cross, which meant that subjects started to explore the scene from its center. Successive
683 fixation locations tend to be close to one another, introducing dependency (Barthelme et al.,
684 2013). Therefore, the fixations that follow the initial, central fixation are also more likely
685 located near the center of the scene. In our data, this showed as the well-known central
686 fixation bias (e.g., Mannan et al., 1996), but note that a central tendency has also been
687 observed for non-central initial fixation positions (Tatler, 2007).

688 In our experiment, subjects had 10 s to look at each scene image, giving them ample
689 time to explore the whole image. An analysis of global eye-movement measures indicated
690 that AMD patients made saccades with shorter amplitudes than age-matched control subjects
691 (Table 2). In the grid GLMM analyses, this translated into a significantly reduced model
692 intercept for the AMD patients, which means that they sampled significantly fewer scene
693 patches than the control subjects (Table 3). Moreover, their central fixation bias was
694 significantly stronger (Table 3, Figure 4). Finally, the results for the by-subject random
695 effects showed a correlation between scene coverage and central bias: The fewer scene
696 patches were selected for fixation, the stronger the central fixation bias (Table 3, Figure 4).

697 The unconstrained nature of our free-viewing task allowed subjects to adopt a
698 viewing style that they deemed fit. AMD patients' less explorative viewing behavior may be
699 due to impairments caused by their scotomata. Note that differences in viewing behavior
700 between AMD patients and age-matched controls are likely to be task dependent. Thibaut et
701 al. (2016) asked AMD patients to name pictures of real-world scenes that were presented for
702 2 s each and found that AMD patients "moved their eyes around more" (p. 88). Thus, AMD
703 patients' explorativeness may depend on the demands imposed by the task at hand.

704 Despite the presence of a central scotoma, AMD patients were more likely to fixate
705 high-salience than low-salience scene patches. This finding is not as counterintuitive as it
706 may seem, given that selection for fixation is essentially a peripheral-vision task (see Ludwig
707 et al., 2014; Nuthmann, 2014). Importantly, the salience effects for the patient group and the
708 control group did not differ in size. At the same time, we found substantial individual
709 differences, in particular in the patient group.

710 Evidence from previous studies suggests that the influence of low-level image
711 features on fixation selection in scenes decreases with increasing age (Açık et al., 2010;
712 Nuthmann et al., 2020). In agreement with this general result, we found that fixation
713 probability was modulated by image salience to a greater extent for young adults than for
714 older adults. We also found that the central bias was (somewhat) less pronounced for young
715 adults, which is different from Nuthmann et al. (2020) who found no differences in central
716 bias for young and older adults. Finally, the distributions of saccade directions indicated
717 subtle differences between young and older adults, warranting further research.

718 In previous investigations, correlations between AMD patients' average scores in a
719 dependent variable of interest and measures of their visual ability were assessed (e.g.,
720 Thibaut et al., 2016; Thibaut et al., 2015; Tran et al., 2010; Wiecek et al., 2012). In the
721 present context, we could have generated the input for such correlation tests by fitting a
722 separate generalized linear model to each subject's data. However, with this approach there is
723 a risk of overfitting the data, because subjects with extreme values are "taken too seriously"
724 (see Gelman & Hill, 2007). Instead, we ran a generalized linear mixed-effects model with by-
725 subject random effects, which allowed us to make predictions for individual subjects in the
726 light of the behavior of all other subjects. In such a model, unreliable between-subject
727 variance in the effects is removed through shrinkage (Efron & Morris, 1977; Makowski et al.,
728 2014; Rouder & Haaf, 2019). It is neither advised nor necessary to correlate the random
729 effects for different subjects with other subject variables such as scotoma size (Kliegl et al.,
730 2011). Instead, patient-related variables can be included as additional fixed-effect terms in
731 the mixed model. Analyzing AMD patients' scene-viewing data this way, we observed a
732 significant interaction between BCEA and visual salience. When fixation stability was low,
733 the impact of visual salience on fixation selection was reduced. By contrast, the size of the
734 lesion did not predict fixation selection in any way.

735 Eye tracking AMD patients is challenging. Calibrating a standard laboratory eye
736 tracker requires subjects to look at a number of calibration targets with known coordinates
737 (see <https://youtu.be/69oriD6j1DI>). Typically, the calibration targets are presented in random
738 order to prevent subjects from anticipating the location of the next target, which may make
739 them leave the current target before it disappears. Given that the calibration procedure
740 requires subjects to saccade to single targets in peripheral vision, the targets need to be
741 visually salient. However, the calibration procedure also requires subjects to fixate each
742 target for a certain amount of time. If AMD patients fixate the target with the fovea, it is
743 obscured by the scotoma. Therefore, some researchers have used a "wagon wheel" as

744 calibration target which is meant to help AMD patients with fixating the target's center of
745 gravity with the fovea (González et al., 2006; Sullivan & Walker, 2015). Alternatively,
746 patients with stable PRLs may use their PRLs rather than their foveae for calibration (see
747 Gupta et al., 2018, for discussion).

748 For eye-tracking studies like ours, it is preferable if subjects approach the fixation
749 task during calibration and the subsequent free-viewing task in similar ways. Therefore,
750 during calibration we neither encouraged foveal fixation by using specifically designed
751 calibration stimuli (Sullivan & Walker, 2015) nor did we specifically encourage the use of a
752 PRL by instructing participants “to look at the target so that it could be seen” (Costela et al.,
753 2017, p. 6074). As indicated in Sec. 2.2 above, we cannot say with certainty whether a given
754 AMD subject used the fovea or a PRL to fixate the calibration targets. In the following, we
755 discuss whether this has any bearing on the interpretation of our empirical findings.

756 In the context of scene viewing, the difference between using the fovea or a pseudo-
757 fovea (PRL) can be described as prioritizing either “seeing” or “looking”. If the patient
758 adopts an eccentric viewing strategy, they will “see” what is at fixation, but their scotoma is
759 likely to hide more eccentric scene content and therefore some of the candidate target
760 locations for the next saccade. Conversely, if the patient does not use a pseudo-fovea, their
761 scotoma will degrade scene information at fixation but leave more scene content visible in
762 the periphery (and thus “to look for”). Either way, the peripheral selection of the target
763 location for the next saccade should follow similar guidance principles as in normally sighted
764 individuals. In agreement with this prediction, we found effects of visual salience on saccade
765 target selection to be preserved in patients with AMD.

766 In principle, more complex scenarios can develop when patients change their fixation
767 behavior, either between the calibration task and the free-viewing task, or within a given task.
768 For example, Costela et al. (2017) compared gaze locations during free-viewing of dynamic
769 scenes (i.e., videos) with the PRL used in a fixation task. The results suggested that people
770 with central vision loss did not necessarily use the same PRL in the two tasks (see also
771 Crossland, Crabb, et al., 2011). Such changes in fixation behavior can result in offsets
772 between measured and actual gaze positions.

773 Note that our grid method is fairly robust in this regard. The scene patches or grid
774 cells that we used for analysis were relatively large in size. Moreover, the mean salience of
775 adjacent scene patches tends to be correlated (see Figure 1d). Finally, we assessed how
776 explorative a subject's viewing behavior was by analyzing the number of scene patches
777 observers selected for fixation. Thus, our analysis method tolerates reductions in accuracy

778 and precision, within limits. We note that other analyses commonly used to investigate eye
779 guidance in scenes place higher demands on accuracy (e.g., Nuthmann, 2017). Therefore, it is
780 important to continue developing methodologies for measuring the location of the PRL (e.g.,
781 Tarita-Nistor et al., 2015) along with eye-tracking technologies that explicitly address the use
782 of a PRL (or sometimes multiple PRLs) instead of the fovea.
783

784

785

Acknowledgements

786 We thank Wolfgang Einhäuser for helpful discussions regarding the grid method.

787

788

References

- 791 Açıık, A., Sarwary, A., Schultze-Kraft, R., Onat, S., & König, P. (2010). Developmental
792 changes in natural viewing behavior: bottom-up and top-down differences between
793 children, young adults and older adults. *Frontiers in Psychology, 1*(11), Article 207.
794 <https://doi.org/10.3389/fpsyg.2010.00207>
- 795 Akaike, H. (1974). A new look at the statistical model identification. *IEEE Transactions on*
796 *Automatic Control, 19*(6), 716-723. <https://doi.org/10.1109/TAC.1974.1100705>
- 797 Altemir, I., Alejandre, A., Fanlo-Zarazaga, A., Ortín, M., Pérez, T., Masiá, B., & Pueyo, V.
798 (2022). Evaluation of fixational behavior throughout life. *Brain Sciences, 12*(1),
799 Article 19. <https://www.mdpi.com/2076-3425/12/1/19>
- 800 Anderson, N. C., Bischof, W. F., Foulsham, T., & Kingstone, A. (2020). Turning the (virtual)
801 world around: Patterns in saccade direction vary with picture orientation and shape in
802 virtual reality. *Journal of Vision, 20*(8), Article 21. <https://doi.org/10.1167/jov.20.8.21>
- 803 Baayen, R. H., Davidson, D. J., & Bates, D. M. (2008). Mixed-effects modeling with crossed
804 random effects for subjects and items. *Journal of Memory and Language, 59*(4), 390-
805 412. <https://doi.org/10.1016/j.jml.2007.12.005>
- 806 Baddeley, R. J., & Tatler, B. W. (2006). High frequency edges (but not contrast) predict
807 where we fixate: A Bayesian system identification analysis. *Vision Research, 46*(18),
808 2824-2833. <https://doi.org/10.1016/j.visres.2006.02.024>
- 809 Barr, D. J., Levy, R., Scheepers, C., & Tily, H. J. (2013). Random effects structure for
810 confirmatory hypothesis testing: Keep it maximal. *Journal of Memory and Language,*
811 *68*(3), 255-278. <https://doi.org/10.1016/j.jml.2012.11.001>
- 812 Barthelme, S., Trukenbrod, H., Engbert, R., & Wichmann, F. (2013). Modeling fixation
813 locations using spatial point processes. *Journal of Vision, 13*(12), Article 1.
814 <https://doi.org/10.1167/13.12.1>
- 815 Bates, D. M., Mächler, M., Bolker, B. M., & Walker, S. (2015). Fitting linear mixed-effects
816 models using lme4. *Journal of Statistical Software, 67*(1), 1-48.
817 <https://doi.org/10.18637/jss.v067.i01>
- 818 Bolker, B. M., Brooks, M. E., Clark, C. J., Geange, S. W., Poulsen, J. R., Stevens, M. H. H.,
819 & White, J.-S. S. (2009). Generalized linear mixed models: a practical guide for
820 ecology and evolution. *Trends in Ecology & Evolution, 24*(3), 127-135.
821 <https://doi.org/10.1016/j.tree.2008.10.008>
- 822 Borji, A., & Itti, L. (2013). State-of-the-art in visual attention modeling. *IEEE Transactions*
823 *on Pattern Analysis and Machine Intelligence, 35*(1), 185-207.
824 <https://doi.org/10.1109/tpami.2012.89>
- 825 Boucart, M., Despretz, P., Hladiuk, K., & Desmettre, T. (2008). Does context or color
826 improve object recognition in patients with low vision? *Visual Neuroscience, 25*(5-6),
827 685-691. <https://doi.org/10.1017/s0952523808080826>
- 828 Boucart, M., Moroni, C., Szaffarczyk, S., & Tran, T. H. C. (2013). Implicit processing of
829 scene context in macular degeneration. *Investigative Ophthalmology & Visual*
830 *Science, 54*(3), 1950-1957. <https://doi.org/10.1167/iovs.12-9680>
- 831 Brown, V. A. (2021). An introduction to linear mixed-effects modeling in R. *Advances in*
832 *Methods and Practices in Psychological Science, 4*(1), 1-19.
833 <https://doi.org/10.1177/2515245920960351>
- 834 Cahill, M. T., Banks, A. D., Stinnett, S. S., & Toth, C. A. (2005). Vision-related quality of
835 life in patients with bilateral severe age related macular degeneration. *Ophthalmology,*
836 *112*(1), 152-158. <https://doi.org/10.1016/j.ophtha.2004.06.036>

- 837 Clarke, A. D. F., & Tatler, B. W. (2014). Deriving an appropriate baseline for describing
838 fixation behaviour. *Vision Research*, 102, 41-51.
839 <https://doi.org/10.1016/j.visres.2014.06.016>
- 840 Costela, F. M., Kajtezovic, S., & Woods, R. L. (2017). The preferred retinal locus used to
841 watch videos. *Investigative Ophthalmology & Visual Science*, 58(14), 6073-6081.
842 <https://doi.org/10.1167/iovs.17-21839>
- 843 Cronbach, L. J. (1957). The two disciplines of scientific psychology. *American Psychologist*,
844 12(5), 671-684. <https://doi.org/10.1037/h0043943>
- 845 Crossland, M. D., Crabb, D. P., & Rubin, G. S. (2011). Task-specific fixation behavior in
846 macular disease. *Investigative Ophthalmology & Visual Science*, 52(1), 411-416.
847 <https://doi.org/10.1167/iovs.10-5473>
- 848 Crossland, M. D., Culham, L. E., & Rubin, G. S. (2004). Fixation stability and reading speed
849 in patients with newly developed macular disease. *Ophthalmic and Physiological*
850 *Optics*, 24(4), 327-333. <https://doi.org/10.1111/j.1475-1313.2004.00213.x>
- 851 Crossland, M. D., Engel, S. A., & Legge, G. E. (2011). The preferred retinal locus in macular
852 disease: toward a consensus definition. *Retina-the Journal of Retinal and Vitreous*
853 *Diseases*, 31(10), 2109-2114. <https://doi.org/10.1097/IAE.0b013e31820d3fba>
- 854 Crossland, M. D., Sims, M., Galbraith, R. F., & Rubin, G. S. (2004). Evaluation of a new
855 quantitative technique to assess the number and extent of preferred retinal loci in
856 macular disease. *Vision Research*, 44(13), 1537-1546.
857 <https://doi.org/10.1016/j.visres.2004.01.006>
- 858 Cummings, R. W., Whittaker, S. G., Watson, G. R., & Budd, J. M. (1985). Scanning
859 characters and reading with a central scotoma. *American Journal of Optometry and*
860 *Physiological Optics*, 62(12), 833-843. <https://doi.org/10.1097/00006324-198512000-00004>
- 861
- 862 David, E. J., Lebranchu, P., Da Silva, M. P., & Le Callet, P. (2019). Predicting artificial
863 visual field losses: A gaze-based inference study. *Journal of Vision*, 19(14), Article
864 22. <https://doi.org/10.1167/19.14.22>
- 865 Demidenko, E. (2013). *Mixed models: Theory and applications with R* (2d ed.). John Wiley
866 & Sons. <https://doi.org/10.1002/9781118651537>
- 867 Efron, B., & Morris, C. (1977). Stein's paradox in statistics. *Scientific American*, 236(5),
868 119-127. <https://doi.org/10.1038/scientificamerican0577-119>
- 869 Foulsham, T., & Kingstone, A. (2010). Asymmetries in the direction of saccades during
870 perception of scenes and fractals: Effects of image type and image features. *Vision*
871 *Research*, 50(8), 779-795. <https://doi.org/10.1016/j.visres.2010.01.019>
- 872 Foulsham, T., Kingstone, A., & Underwood, G. (2008). Turning the world around: Patterns
873 in saccade direction vary with picture orientation. *Vision Research*, 48(17), 1777-
874 1790. <https://doi.org/10.1016/j.visres.2008.05.018>
- 875 Frintrop, S., Rome, E., & Christensen, H. I. (2010). Computational visual attention systems
876 and their cognitive foundations: A survey. *ACM Transactions on Applied Perception*,
877 7(1), Article 6. <https://doi.org/10.1145/1658349.1658355>
- 878 Garcia-Diaz, A., Leborán, C., Fdez-Vidal, X. R., & Pardo, X. M. (2012). On the relationship
879 between optical variability, visual saliency, and eye fixations: A computational
880 approach. *Journal of Vision*, 12(6), Article 17. <https://doi.org/10.1167/12.6.17>
- 881 Gelman, A., & Hill, J. (2007). *Data analysis using regression and multilevel/hierarchical*
882 *models*. Cambridge University Press.
- 883 González, E. G., Teichman, J., Lillakas, L., Markowitz, S. N., & Steinbach, M. J. (2006).
884 Fixation stability using radial gratings in patients with age-related macular
885 degeneration. *Canadian Journal of Ophthalmology-Journal Canadien*
886 *d'Ophthalmologie*, 41(3), 333-339. <https://doi.org/10.1139/i06-019>

- 887 Gupta, A., Mesik, J., Engel, S. A., Smith, R., Schatza, M., Calabrese, A., van Kuijk, F. J.,
888 Erdman, A. G., & Legge, G. E. (2018). Beneficial effects of spatial remapping for
889 reading with simulated central field loss. *Investigative Ophthalmology & Visual
890 Science*, 59(2), 1105-1112. <https://doi.org/10.1167/iovs.16-21404>
- 891 Hohenstein, S., & Kliegl, R. (2020). *remef: Remove partial effects*. In (*R package version
892 1.0.7*). <https://github.com/hohenstein/remef/>
- 893 Itti, L., Koch, C., & Niebur, E. (1998). A model of saliency-based visual attention for rapid
894 scene analysis. *IEEE Transactions on Pattern Analysis and Machine Intelligence*,
895 20(11), 1254-1259. <https://doi.org/10.1109/34.730558>
- 896 Jaeger, T. F. (2008). Categorical data analysis: Away from ANOVAs (transformation or not)
897 and towards logit mixed models. *Journal of Memory and Language*, 59(4), 434-446.
898 <https://doi.org/10.1016/j.jml.2007.11.007>
- 899 Kliegl, R., Wei, P., Dambacher, M., Yan, M., & Zhou, X. (2011). Experimental effects and
900 individual differences in linear mixed models: estimating the relationship between
901 spatial, object, and attraction effects in visual attention. *Frontiers in Psychology*, 1,
902 Article 238. <https://doi.org/10.3389/fpsyg.2010.00238>
- 903 Kumar, G., & Chung, S. T. L. (2014). Characteristics of fixational eye movements in people
904 with macular disease. *Investigative Ophthalmology & Visual Science*, 55(8), 5125-
905 5133. <https://doi.org/10.1167/iovs.14-14608>
- 906 Kuznetsova, A., Brockhoff, P. B., & Christensen, R. H. B. (2017). lmerTest Package: Tests in
907 Linear Mixed Effects Models. *Journal of Statistical Software*, 82(13), 1-26.
908 <https://doi.org/10.18637/jss.v082.i13>
- 909 Loschky, L. C., Szaffarczyk, S., Beugnet, C., Young, M. E., & Boucart, M. (2019). The
910 contributions of central and peripheral vision to scene-gist recognition with a 180°
911 visual field. *Journal of Vision*, 19(5), Article 15. <https://doi.org/10.1167/19.5.15>
- 912 Ludwig, C. J. H., Davies, J. R., & Eckstein, M. P. (2014). Foveal analysis and peripheral
913 selection during active visual sampling. *Proceedings of the National Academy of
914 Sciences of the United States of America*, 111(2), E291-E299.
915 <https://doi.org/10.1073/pnas.1313553111>
- 916 Makowski, S., Dietz, A., & Kliegl, R. (2014). Shrinkage—application and tutorial.
917 <https://doi.org/10.5281/zenodo.11172>
- 918 Malcolm, G. L., Groen, I. I. A., & Baker, C. I. (2016). Making sense of real-world scenes.
919 *Trends in Cognitive Sciences*, 20(11), 843-856.
920 <https://doi.org/10.1016/j.tics.2016.09.003>
- 921 Mannan, S. K., Ruddock, K. H., & Wooding, D. S. (1996). The relationship between the
922 locations of spatial features and those of fixations made during visual examination of
923 briefly presented images. *Spatial Vision*, 10(3), 165-188.
924 <https://doi.org/10.1163/156856896X00123>
- 925 Nuthmann, A. (2014). How do the regions of the visual field contribute to object search in
926 real-world scenes? Evidence from eye movements. *Journal of Experimental
927 Psychology: Human Perception and Performance*, 40(1), 342-360.
928 <https://doi.org/10.1037/a0033854>
- 929 Nuthmann, A. (2017). Fixation durations in scene viewing: Modeling the effects of local
930 image features, oculomotor parameters, and task. *Psychonomic Bulletin & Review*,
931 24(2), 370-392. <https://doi.org/10.3758/s13423-016-1124-4>
- 932 Nuthmann, A., Clayden, A. C., & Fisher, R. B. (2021). The effect of target salience and size
933 in visual search within naturalistic scenes under degraded vision. *Journal of Vision*,
934 21(4), Article 2. <https://doi.org/10.1167/jov.21.4.2>

- 935 Nuthmann, A., & Einhäuser, W. (2015). A new approach to modeling the influence of image
936 features on fixation selection in scenes. *Annals of the New York Academy of Sciences*,
937 1339(1), 82-96. <https://doi.org/10.1111/nyas.12705>
- 938 Nuthmann, A., Einhäuser, W., & Schütz, I. (2017). How well can saliency models predict
939 fixation selection in scenes beyond central bias? A new approach to model evaluation
940 using generalized linear mixed models. *Frontiers in Human Neuroscience*, 11(10),
941 Article 491. <https://doi.org/10.3389/fnhum.2017.00491>
- 942 Nuthmann, A., & Henderson, J. M. (2010). Object-based attentional selection in scene
943 viewing. *Journal of Vision*, 10(8), Article 20. <https://doi.org/10.1167/10.8.20>
- 944 Nuthmann, A., Schütz, I., & Einhäuser, W. (2020). Saliency-based object prioritization
945 during active viewing of naturalistic scenes in young and older adults. *Scientific*
946 *Reports*, 10(1), Article 22057. <https://doi.org/10.1038/s41598-020-78203-7>
- 947 Parkhurst, D., Law, K., & Niebur, E. (2002). Modeling the role of saliency in the allocation
948 of overt visual attention. *Vision Research*, 42(1), 107-123.
949 [https://doi.org/10.1016/S0042-6989\(01\)00250-4](https://doi.org/10.1016/S0042-6989(01)00250-4)
- 950 Peters, R. J., Iyer, A., Itti, L., & Koch, C. (2005). Components of bottom-up gaze allocation
951 in natural images. *Vision Research*, 45(18), 2397-2416.
952 <https://doi.org/10.1016/j.visres.2005.03.019>
- 953 Querques, G., Tran, T. H. C., Forte, R., Querques, L., Bandello, F., & Souied, E. H. (2012).
954 Anatomic response of occult choroidal neovascularization to intravitreal ranibizumab:
955 a study by indocyanine green angiography. *Graefes Archive for Clinical and*
956 *Experimental Ophthalmology*, 250(4), 479-484. <https://doi.org/10.1007/s00417-011-1831-5>
- 957
- 958 Rabbitt, P. (1993). Does it all go together when it goes? *Quarterly Journal of Experimental*
959 *Psychology Section a-Human Experimental Psychology*, 46(3), 385-434.
960 <https://doi.org/10.1080/14640749308401055>
- 961 Rohrschneider, K., Becker, M., Kruse, F. E., Fendrich, T., & Völcker, H. E. (1995). Stability
962 of fixation: results of fundus-controlled examination using the scanning laser
963 ophthalmoscope. *German Journal of Ophthalmology*, 4(4), 197-202.
- 964 Rothkegel, L. O. M., Trukenbrod, H. A., Schütt, H. H., Wichmann, F. A., & Engbert, R.
965 (2017). Temporal evolution of the central fixation bias in scene viewing. *Journal of*
966 *Vision*, 17(13), Article 3. <https://doi.org/10.1167/17.13.3>
- 967 Rouder, J. N., & Haaf, J. M. (2019). A psychometrics of individual differences in
968 experimental tasks. *Psychonomic Bulletin & Review*, 26(2), 452-467.
969 <https://doi.org/10.3758/s13423-018-1558-y>
- 970 Rubin, G. S. (2013). Measuring reading performance. *Vision Research*, 90, 43-51.
971 <https://doi.org/10.1016/j.visres.2013.02.015>
- 972 Rubin, G. S., & Feely, M. (2009). The role of eye movements during reading in patients with
973 age-related macular degeneration (AMD). *Neuro-Ophthalmology*, 33(3), 120-126.
974 <https://doi.org/10.1080/01658100902998732>
- 975 Salvucci, D. D., & Goldberg, J. H. (2000). Identifying fixations and saccades in eye-tracking
976 protocols. *Proceedings of the Symposium on Eye Tracking Research and*
977 *Applications*, 71-78. <https://doi.org/10.1145/355017.355028>
- 978 Schielzeth, H., & Forstmeier, W. (2009). Conclusions beyond support: overconfident
979 estimates in mixed models. *Behavioral Ecology*, 20(2), 416-420.
980 <https://doi.org/10.1093/beheco/arn145>
- 981 Schwarz, G. (1978). Estimating the dimension of a model. *The Annals of Statistics*, 6(2), 461-
982 464. <https://doi.org/10.1214/aos/1176344136>

- 983 Seghier, M. L., & Price, C. J. (2018). Interpreting and utilising intersubject variability in
984 brain function. *Trends in Cognitive Sciences*, 22(6), 517-530.
985 <https://doi.org/10.1016/j.tics.2018.03.003>
- 986 Shammi, P., Bosman, E., & Stuss, D. T. (1998). Aging and variability in performance. *Aging*
987 *Neuropsychology and Cognition*, 5(1), 1-13. <https://doi.org/10.1076/anec.5.1.1.23>
- 988 Staub, A. (2020). Do effects of visual contrast and font difficulty on readers' eye movements
989 interact with effects of word frequency or predictability? *Journal of Experimental*
990 *Psychology: Human Perception and Performance*, 46(11), 1235-1251.
991 <https://doi.org/10.1037/xhp0000853>
- 992 Steinman, R. M. (1965). Effect of target size luminance and color on monocular fixation.
993 *Journal of the Optical Society of America*, 55(9), 1158-1165.
994 <https://doi.org/10.1364/josa.55.001158>
- 995 Sullivan, B., & Walker, L. (2015). Comparing the fixational and functional preferred retinal
996 location in a pointing task. *Vision Research*, 116, 68-79.
997 <https://doi.org/10.1016/j.visres.2015.07.007>
- 998 Tarita-Nistor, L., Eizenman, M., Landon-Brace, N., Markowitz, S. N., Steinbach, M. J., &
999 González, E. G. (2015). Identifying absolute preferred retinal locations during
1000 binocular viewing. *Optometry and Vision Science*, 92(8), 863-872.
1001 <https://doi.org/10.1097/opx.0000000000000641>
- 1002 Tatler, B. W. (2007). The central fixation bias in scene viewing: Selecting an optimal
1003 viewing position independently of motor biases and image feature distributions.
1004 *Journal of Vision*, 7(14), Article 4. <https://doi.org/10.1167/7.14.4>
- 1005 Tatler, B. W., Baddeley, R. J., & Gilchrist, I. D. (2005). Visual correlates of fixation
1006 selection: effects of scale and time. *Vision Research*, 45(5), 643-659.
1007 <https://doi.org/10.1016/j.visres.2004.09.017>
- 1008 Taylor, D. J., Hobby, A. E., Binns, A. M., & Crabb, D. P. (2016). How does age-related
1009 macular degeneration affect real-world visual ability and quality of life? A systematic
1010 review. *BMJ Open*, 6(12), Article e011504. [https://doi.org/10.1136/bmjopen-2016-](https://doi.org/10.1136/bmjopen-2016-011504)
1011 [011504](https://doi.org/10.1136/bmjopen-2016-011504)
- 1012 Thibaut, M., Boucart, M., & Tran, T. H. C. (2020). Object search in neovascular age-related
1013 macular degeneration: the crowding effect. *Clinical and Experimental Optometry*,
1014 103(5), 648-655. <https://doi.org/10.1111/cxo.12982>
- 1015 Thibaut, M., Delerue, C., Boucart, M., & Tran, T. H. C. (2016). Visual exploration of objects
1016 and scenes in patients with age-related macular degeneration. *Journal Français*
1017 *d'Ophthalmologie*, 39(1), 82-89. <https://doi.org/10.1016/j.jfo.2015.08.010>
- 1018 Thibaut, M., Tran, T. H. C., Delerue, C., & Boucart, M. (2015). Misidentifying a tennis
1019 racket as keys: object identification in people with age-related macular degeneration.
1020 *Ophthalmic and Physiological Optics*, 35(3), 336-344.
1021 <https://doi.org/10.1111/opo.12201>
- 1022 Timberlake, G. T., Mainster, M. A., Peli, E., Augliere, R. A., Essock, E. A., & Arend, L. E.
1023 (1986). Reading with a macular scotoma. I. Retinal location of scotoma and fixation
1024 area. *Investigative Ophthalmology & Visual Science*, 27(7), 1137-1147.
- 1025 Tran, T. H. C., Despretz, P., & Boucart, M. (2012). Scene perception in age-related macular
1026 degeneration: the effect of contrast. *Optometry and Vision Science*, 89(4), 419-425.
1027 <https://doi.org/10.1097/OPX.0b013e31824c3a21>
- 1028 Tran, T. H. C., Rambaud, C., Despretz, P., & Boucart, M. (2010). Scene perception in age-
1029 related macular degeneration. *Investigative Ophthalmology & Visual Science*, 51(12),
1030 6868-6874. <https://doi.org/10.1167/iovs.10-5517>

1031 Van Renswoude, D. R., Johnson, S. P., Raijmakers, M. E. J., & Visser, I. (2016). Do infants
1032 have the horizontal bias? *Infant Behavior & Development*, 44, 38-48.
1033 <https://doi.org/10.1016/j.infbeh.2016.05.005>

1034 Verghese, P., Vullings, C., & Shandize, N. (2021). Eye movements in macular degeneration.
1035 *Annual Review of Vision Science*, 7, 773-791. [https://doi.org/10.1146/annurev-vision-](https://doi.org/10.1146/annurev-vision-100119-125555)
1036 [100119-125555](https://doi.org/10.1146/annurev-vision-100119-125555)

1037 Vogel, E. K., & Awh, E. (2008). How to exploit diversity for scientific gain: Using individual
1038 differences to constrain cognitive theory. *Current Directions in Psychological*
1039 *Science*, 17(2), 171-176. <https://doi.org/10.1111/j.1467-8721.2008.00569.x>

1040 Vullings, C., & Verghese, P. (2021). Mapping the binocular scotoma in macular
1041 degeneration. *Journal of Vision*, 21(3), Article 9. <https://doi.org/10.1167/jov.21.3.9>

1042 Wickham, H. (2016). *ggplot2: Elegant graphics for data analysis* (2d ed.). Springer.
1043 <https://doi.org/10.1007/978-3-319-24277-4>

1044 Wiecek, E., Jackson, M. L., Dakin, S. C., & Bex, P. (2012). Visual search with image
1045 modification in age-related macular degeneration. *Investigative Ophthalmology &*
1046 *Visual Science*, 53(10), 6600-6609. <https://doi.org/10.1167/iovs.12-10012>

1047 Wilke, C. O. (2020). *Cowplot: Streamlined plot theme and plot annotations for 'ggplot2'*. In
1048 (*R package version 1.1.1*). <https://CRAN.R-project.org/package=cowplot>

1049 Wilkinson, G. N., & Rogers, C. E. (1973). Symbolic description of factorial models for
1050 analysis of variance. *The Royal Statistical Society Series C-Applied Statistics*, 22(3),
1051 392-399. <https://doi.org/10.2307/2346786>

1052 Wloka, C., Kunić, T., Kotseruba, I., Fahimi, R., Frosst, N., Bruce, N. D. B., & Tsotsos, J. K.
1053 (2018). SMILER: Saliency model implementation library for experimental research.
1054 *arXiv preprint*. <https://doi.org/10.48550/arXiv.1812.08848>

1055 Wolfers, T., Beckmann, C. F., Hoogman, M., Buitelaar, J. K., Franke, B., & Marquand, A. F.
1056 (2020). Individual differences v. the average patient: mapping the heterogeneity in
1057 ADHD using normative models. *Psychological Medicine*, 50(2), 314-323.
1058 <https://doi.org/10.1017/s0033291719000084>

1059 Zhaoping, L. (2019). A new framework for understanding vision from the perspective of the
1060 primary visual cortex. *Current Opinion in Neurobiology*, 58, 1-10.
1061 <https://doi.org/10.1016/j.conb.2019.06.001>
1062
1063

1064
1065
1066
1067
1068
1069
1070
1071
1072
1073
1074

Footnotes

¹ Visual cognition researchers typically consider central vision to be from 0° to 5° eccentricity; everything beyond 5° is peripheral vision (Loschky et al., 2019).

² There was one exception: When using the binary response variable and a 6 × 4 grid, the model intercept was significantly larger for young compared with old subjects. In our main analysis, this difference was not significant (Table 3, Figure 3a).

³ In both of these additional GLMMs, the fixed-effect coefficients for the intercept, the central bias, and salience were significantly different from zero, as would be expected from the results of the main GLMM (Table 3).

1075
1076
1077
1078
1079

Tables

Table 1. Individual demographic and clinical data for the AMD patients included in the study.

Participant Number	Gender	Age	MMSE score	Duration of AMD (months)	Visual acuity (LogMAR)	GLD (mm)	SA (mm ²)	BCEA (minarc ²)
1	female	82	27	42.4	0.6	3.417	6.97	3120.71
2	female	78	28	45.7	0.4	3.058	4.8	2340.08
3	female	82	30	76.1	0.4	2.925	4.91	3253.23
4	female	72	30	74.2	1	3.375	8.9	8779.51
5	female	80	29	13.8	0.8	3.532	9.57	5555.60
6	male	83	28	14.4	0.4	2.586	2.82	1883.36
7	female	80	30	3	1.6	6.525	25.74	11394.56
8	female	78	28	27.3	0.4	1.623	1.39	16657.36
9	female	77	30	7.5	0.6	2.831	4.21	1349.14
10	female	81	30	73.2	1	5.896	21.21	13908.58
11	female	79	30	7.9	0.4	0.384	0.04	13542.71
12	female	71	29	9.1	0.3	1.758	2.83	17492.23
13	female	81	30	60	0.8	4.910	9.79	16903.14
14	male	86	30	41	0.3	0.855	0.42	9249.95
15	female	74	27	1.8	0.7	3.006	5.3	11162.78
16	female	73	30	98	0.4	2.669	3.64	900.34
17	male	73	26	41	0.9	4.681	10.65	11057.94

1080 *Note.* MMSE = Mini Mental State Examination, AMD = age-related macular degeneration,
1081 LogMAR = logarithm of the minimum angle of resolution, GLD = greatest linear diameter of
1082 the lesion, SA = surface area, BCEA = bivariate contour ellipse area.

1083

1084

1085 Table 2. Mean (and standard deviation) general scanning behavior per participant for AMD
1086 patients, age-matched normally sighted subjects, and young adults.

1087

		Number of	Fixation	Saccade
		fixations per trial	duration (ms)	amplitude (°)
	AMD patients	30.35 (9.1)	233.93 (97.3)	3.18 (1.05)
Subject group	older adults	30.52 (5.61)	241.46 (64.38)	4.6 (1.19)
	young adults	29.5 (5.37)	270 (84.79)	5.1 (1.25)

1088

1089

1090 Table 3. Generalized linear mixed model fitting the effect of image salience and central bias
 1091 on fixation probability in scene viewing: estimates of coefficients (*b*), standard errors (*SE*), *z*-
 1092 values, and *p*-values for fixed effects and variances and correlations for random effects.

1093

<i>Fixed Effects</i>				
	<i>B</i>	<i>SE</i>	<i>z</i>	<i>p</i>
Intercept (Old)	-2.0495	0.1218	-16.827	< 0.001
Intercept: AMD - Old	-0.8298	0.1645	-5.045	< 0.001
Intercept: Young - Old	0.2911	0.162	1.797	0.072
Central bias (Old)	-0.772	0.0944	-8.175	< 0.001
Central bias: AMD - Old	-0.534	0.1282	-4.165	< 0.001
Central bias: Young - Old	0.2561	0.1263	2.028	0.043
Saliency (Old)	0.245	0.072	3.401	0.001
Saliency: AMD - Old	-0.0077	0.0797	-0.097	0.923
Saliency: Young - Old	0.2497	0.0787	3.171	0.002
<i>Random Effects</i>				
Groups	Name	Variance	Correlation	
Subject	Intercept	0.21583	Intercept	
	Central bias	0.12932	0.74	Central bias
	Saliency	0.04866	-0.11	-0.15
Scene	Intercept	0.03314	Intercept	
	Central bias	0.01780	0.50	Central bias
	Saliency	0.04069	0.25	0.43

1094